Reaction pathway and free energy barrier for defect-induced water dissociation on the (101) surface of TiO_2-anatase

Cite as: J. Chem. Phys. **119**, 7445 (2003); https://doi.org/10.1063/1.1607306
Submitted: 21 April 2003 . Accepted: 17 July 2003 . Published Online: 26 September 2003

Antonio Tilocca, and Annabella Selloni

Reaction pathway and free energy barrier for defect-induced water dissociation on the (101) surface of TiO_2-anatase

Antonio Tilocca[a] and Annabella Selloni
Department of Chemistry, Princeton University, Princeton, New Jersey 08544

(Received 21 April 2003; accepted 17 July 2003)

The adsorption of a water molecule on a partially reduced TiO_2 anatase (101) surface has been studied by first-principles molecular-dynamics simulations. At variance with the stoichiometric surface, dissociation of water close to the oxygen vacancy is energetically favored compared to molecular adsorption. However, no spontaneous dissociation was observed in a simulation of several picoseconds, indicating the presence of an energy barrier between the molecular and dissociated states. The free energy profile along a possible dissociation path has been determined through constrained molecular dynamics runs, from which a free energy barrier for dissociation of ~0.1 eV is estimated. On the basis of these results, a mechanism for the dissociation of water at low coverage is proposed. © *2003 American Institute of Physics*. [DOI: 10.1063/1.1607306]

I. INTRODUCTION

The adsorption and reactivity of water on TiO_2 surfaces is an essential aspect of many applications of this material. In particular, water–surface interactions play a key role in photocatalytic processes like hydrogen production[1] and decontamination of polluted water.[1–3] A central issue in understanding these processes is the nature of water adsorption, i.e., whether water is adsorbed in molecular or dissociated form.[4] The surface hydroxyl groups produced by dissociation change the chemical properties of the surface. For instance, a recent study has shown that bridging OH groups are directly involved in scavenging photoexcited electrons by reacting with molecular oxygen, and molecular water hydrogen-bonded to surface OH groups may negatively affect this process by preventing access of O_2 to the hydroxyl groups.[5] Many experimental,[6,7] and theoretical[8–11] studies have addressed the nature of water adsorption on rutile $TiO_2(110)$. However the picture remained controversial until recent scanning tunneling microscopy (STM) experiments,[12,13] supported by density-functional theory (DFT) calculations,[13] clearly showed that, at low coverage, water dissociation on the rutile (110) surface occurs exclusively on oxygen vacancies.

Although the anatase polymorph of TiO_2 is known to be more active than rutile for several photocatalytic applications,[14] so far only a few studies of water–anatase surface interactions have been published. For the most stable anatase (101) surface,[15] DFT calculations found that, irrespective of coverage, molecular adsorption is always favored in the absence of defects.[16] This result is consistent with recent temperature-programmed desorption (TPD) and x-ray photoelectron spectroscopy (XPS) experiment,[17] which found that the adsorbed water is predominantly bound to the surface in a molecular state on anatase (101).

Similarly to rutile (110), the anatase (101) surface shows both fully coordinated ($6c$) and under-coordinated ($5c$) Ti atoms, as well as threefold ($3c$) and twofold ($2c$) coordinated oxygens. Compared to rutile, the surface of anatase shows less tendency to form oxygen vacancies,[18] presumably because the removal of a bridging oxygen leads to the formation of a fourfold coordinated titanium atom (Ti_{4c}), which is less stable than the Ti_{5c} sites formed at oxygen vacancies on rutile (110).[17] However, undercoordinated Ti_{4c} sites are actually present at the step edges of anatase (101). Such sites have been experimentally identified by STM[18] and found to play an important role in the chemistry of this surface.[17,18]

To obtain insight into the role of low-coordinated defect sites in the surface chemistry of anatase, and, more generally, of titania surfaces, in this paper we study the adsorption of a H_2O molecule on partially reduced anatase (101) using first-principles Car–Parrinello molecular dynamics (CPMD) simulations.[19] A few investigations of water on defect-free and defective oxide surfaces have been already carried out using this approach.[9,10,20–24] For instance, spontaneous dissociation of water on defect-free rutile $TiO_2(110)$ was reported to occur in CPMD trajectories at 500 K.[9] In a subsequent study,[21] however, molecular water was found to be stable at 350 K on the (110) surface, whereas spontaneous dissociation was observed at oxygen vacancies of the defective $TiO_2(100)$ surface. Other CPMD investigations showed that isolated water molecules spontaneously dissociate at defective MgO (100) surfaces, but not on the defect-free surface.[20] In more recent work,[10,24] mixed molecular–dissociated water layers have been reported to occur on both $TiO_2(110)$ and MgO(100) at high coverages. Altogether, these studies show that CPMD simulations undoubtedly represent a powerful tool to explore sorbate dynamics on surfaces. However, since the accessible time scales are still very limited, the dynamical simulations should be complemented by structural optimizations as well as calculation of (free) energy barriers.[22,23]

[a]Electronic mail: atilocca@princeton.edu

II. COMPUTATIONAL APPROACH

Calculations have been performed using the Perdew–Burke–Ernzerhof (PBE)[25] functional for the exchange-correlation term of the electron–electron interaction. The use of a gradient corrected functional is essential to obtain a reliable description of hydrogen bonds and water–surface intermolecular interactions; in addition, the PBE functional has been shown to perform well for bulk and surface TiO_2 anatase.[15] Vanderbilt ultrasoft[26] pseudopotentials have been used to describe electron–core interactions, and valence electrons included the O $2s$, $2p$ and Ti $3s$, $3p$, $3d$, $4s$ shells. The smooth part of the wave functions was expanded in plane waves up to a kinetic-energy cutoff of 25 Ry, while the augmented density cutoff was 200 Ry. The large size of the periodic supercell (see below) allowed us to restrict the k-sampling to the Γ point. All these approximations have been extensively tested, and found adequate in previous studies of titania surfaces.[15,16,27,28] We modeled the anatase surface using a supercell approach; each supercell exposes a surface area of 10.24×11.36 Å^2 (corresponding to three surface cells of the undefected surface), and includes a periodically repeated slab of four Ti_6O_{12} layers, corresponding to a thickness of ~6 Å. We checked that geometries and adsorption energies do not change significantly if they are calculated using a thicker slab.[27,28] The slabs are separated by a vacuum region of ~10 Å along the perpendicular direction. A point defect was created by removing a bridging oxygen from the top layer, so that the net composition of the supercell (without water) is $Ti_{24}O_{47}$. A rather large surface cell is needed here to effectively isolate the defect, by minimizing the interaction with its periodic replicas. The optimized slab geometry is shown in Fig. 1. A water molecule was adsorbed on the top layer only, while the atoms of the bottom layer were fixed in their bulk positions. Geometry optimizations were carried out through damped dynamics until every component of the ionic forces was less than 0.05 eV/Å. In each case, the initial configuration was heated to ~400 K and then left free to evolve in a short MD run; a low potential energy configuration during such run was used as the starting point for the damped dynamics. At the end of the minimization, additional MD runs were carried out to test the stability of the optimized structure.

In most simulations, a fictitious electronic mass $\mu=500$ a.u. and a time step $\delta t=5$ a.u. (0.121 fs) were used, together with the "true" hydrogen mass of 1 amu. With these parameters, the total energy was well conserved in all trajectories where water remained undissociated. Instead, instabilities occurred in the case of dissociation, probably connected to the fast electronic rearrangements brought about by the process, as well as to the low energy gap between occupied and empty electronic states typical of partially reduced TiO_2 surfaces.[29–31] Therefore, more conservative parameters ($\delta t=4$ a.u., hydrogen mass=2 amu, and $\mu=700$ a.u.) were chosen for studying the dissociation dynamics. MD trajectories were run at an average temperature around 300 K (RT). Although TPD experiments[17] show that the desorption temperature of water coordinated to Ti_{5c} is ~250 K, in our simulations the water molecule is coordinated to Ti_{4c}, with a much larger binding energy (see below). Indeed no desorption has been observed throughout the calculated trajectories of this work.

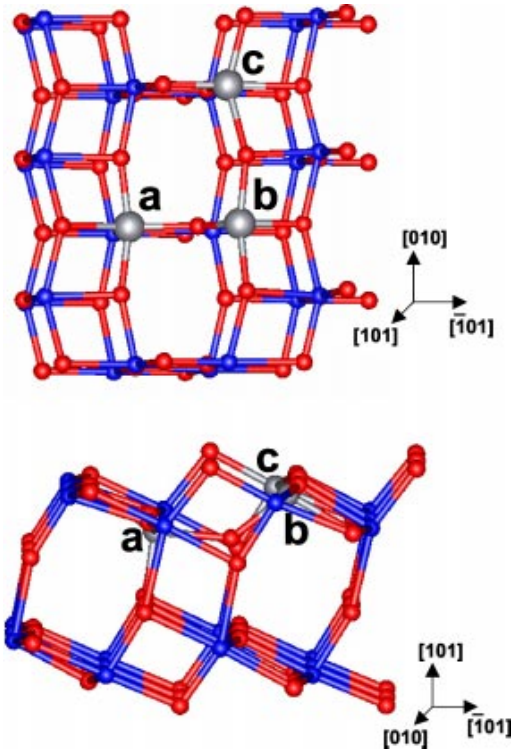

FIG. 1. (top) The defective anatase (101) slab used in the calculations (optimized geometry). The three undercoordinated titanium ions considered as possible adsorption sites are shown as large gray spheres. Atoms a and c are fivefold coordinated, while (b) is fourfold coordinated. (bottom) Side view of the same structure. Note the upward relaxation of the oxygen atom below the vacancy.

III. RESULTS

A. Molecularly versus dissociatively adsorbed water: Structure and energetics

The stoichiometric anatase (101) surface has a corrugated profile, showing alternate rows of Ti_{6c}, O_{2c}, Ti_{5c}, and O_{3c} running along [010] (Fig. 1). On this surface, water adsorbs in molecular form,[16] with the oxygen atom above a Ti_{5c} site, and the hydrogens forming H-bonds with two surface O_{2c} atoms. When the surface is partially reduced by removal of an O_{2c}, the Ti_{6c} and Ti_{5c} atoms to which this bridging oxygen was originally coordinated turn into fivefold (Ti_{5c}) and fourfold coordinated (Ti_{4c}) sites, respectively. We started our study of molecular water adsorption close to the vacancy, by successively placing the molecule above these undercoordinated Ti sites [Figs. 1(a) and 1(b)], as well as above an additional Ti_{5c} atom [Fig. 1(c)]. The final, optimized structures—that we shall call M1, M2, M3—are shown in Fig. 2, together with their corresponding adsorption energies. A further starting geometry with the water oxygen roughly replacing the missing surface O_{2c} converged to the same final state as M2. It appears that the chemisorption on Ti_{4c} is much stronger than on Ti_{5c}. The most stable structure is M2, with the water oxygen bonded to Ti_{4c} and the two

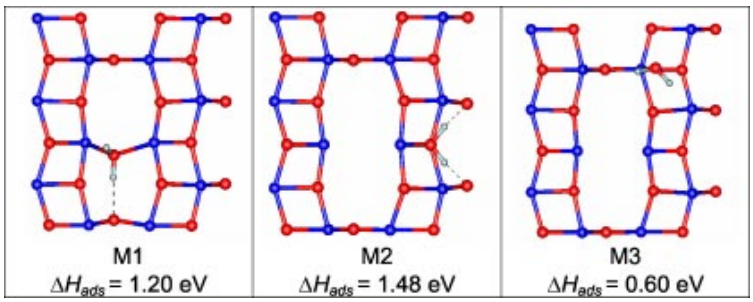

FIG. 2. Optimized geometries of molecular water close to the vacancy. The reported adsorption energies are calculated as $\Delta H_{ads} = -[E_{tot} - E_{bare} - E_{wat}]$, where $E_{tot}(E_{bare})$ are the energy of the slab with (without) adsorbate and E_{wat} is the energy of an isolated water molecule calculated in the same supercell.

hydrogens forming strong H-bonds ($R_{H-O2c} = 1.81$ Å) with two surface bridging oxygens. Structure M1, in which water is coordinated to both Ti_{4c} and Ti_{5c} and forms a weaker H-bond with an O_{2c} ($R_{H-O2c} = 2$ Å) has a somewhat smaller adsorption energy. The water oxygen in M1 roughly replaces the missing O_{2c}; the stabilization resulting from restoring the coordination shell of two surface titania is counterbalanced by a less effective arrangement of the hydrogen atoms compared to M2. In the latter, a small shift of the molecule away from the vacancy allows the formation of two strong hydrogen bonds with the surface. Moreover, in M2 the bond between the surface Ti_{4c} atom and the water oxygen is much stronger than the two Ti–O bonds in M1, as shown by the corresponding bondlengths, 2.11 Å for the Ti_{4c}–O bondlength in M2 versus 2.32 and 2.55 Å for the Ti_{4c}–O and Ti_{5c}–O bondlengths in M1. Finally, the adsorption energy of a water molecule bonded only to Ti_{5c} (M3) is much lower, and close to the 0.74 eV value for Ti_{5c}-coordinated water on the stoichiometric surface.[16]

Structures with dissociated water were generated starting from M1 and M2 and moving a water proton to the H-bonded O_{2c}. The corresponding energy-minimized structures are shown in Fig. 3. The D1 geometry originated from M1 shows two bridging hydroxyl groups (OH_b) and no H-bonds; this structure is more stable than the one (labeled D2) obtained by dissociation of M2, featuring one OH_b and one terminal hydroxyl (OH_t). This is not surprising, as singly coordinated hydroxyl groups are expected to be less stable than bridging ones.[12,21] Indeed, when a RT molecular dynamics simulation was started from D2, the OH_t bonded to Ti_{4c} gradually migrated towards the vacancy in a bridging position between Ti_{4c} and Ti_{5c} (structure D3), where it remained stable during a 1.5 ps trajectory. Optimization of this geometry led to an adsorption energy of 1.85 eV, essentially the same as that of D1. Other possible dissociated configurations were also considered, but found to be substantially less stable than those in Fig. 3.

In summary, similarly to what was found for rutile $TiO_2(110)$,[12,13] at an oxygen vacancy of the anatase (101) surface dissociative adsorption of water is thermodynamically favored with respect to molecular adsorption. The stability of the dissociated configurations D1 and D3 was further tested by running RT simulations; no recombination to molecular water was observed in 1.5 ps.

B. Dissociation pathway and barrier

On the basis of the calculated molecular and dissociated configurations for adsorbed water, a direct dissociation path linking M1 with D1 seems plausible. However, we never observed a dissociation of this type in our molecular dynamics simulations, and found rather that M1 transforms to the other, more stable, molecular structure M2. (This occurs in a time of ~1.5 ps at RT: In the first picosecond the H-bond is broken and the water molecule moves along [010] forming a new H-bond with the O_{2c} on the opposite side of the vacancy. Then this H-bond is broken as well, and the molecule migrates along $[\bar{1}01]$, ending with its two hydrogen pointing towards the two O_{2c}'s, as in M2.) Thus, M2 is the most appropriate starting point for studying the dissociation. However, starting from M2, the molecule only showed local oscillation about the adsorption site, with no dissociation in a simulation of 6 ps. This suggests the presence of an energy barrier to the dissociation, larger than the thermal energy at 300 K.

In order to identify a possible reaction path for the activated dissociation, we used the *Blue Moon* ensemble method,[32,33] and took the distance between the transferred

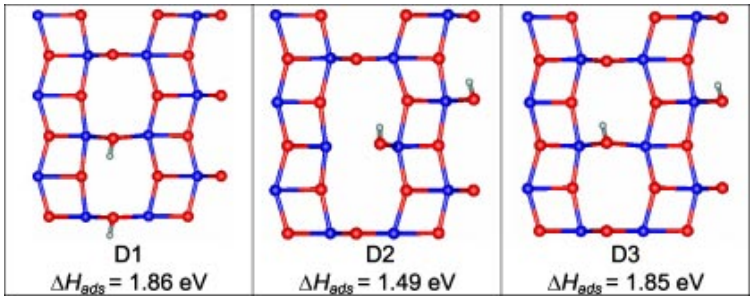

FIG. 3. Optimized geometries of dissociated water close to the vacancy. D1 and D2 are obtained after moving one proton of M1 and M2, respectively, to the H-bonded surface bridging oxygen. D3 is obtained after reoptimizing the final configuration of an MD trajectory started from D2.

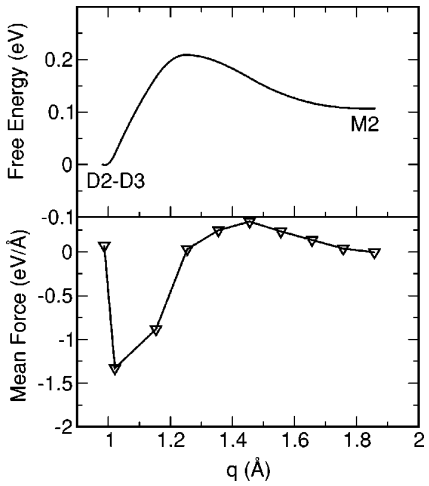

FIG. 4. Free energy profile (top) and mean constaint force (bottom) along the reaction coordinate q. Labels as in Figs. 2 and 3.

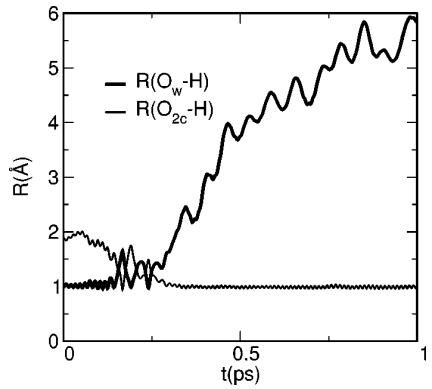

FIG. 5. Time dependence of the O_wH (thick line) and $O_{2c}H$ (thin line) bond distances, following heating of the system to 700 K.

proton and the target surface O_{2c} as the reaction coordinate (q in the following). Ten constrained simulations were carried out. In each trajectory, q was constrained to a fixed value and after a short equilibration the running average of the constraint force was calculated until it converged to a constant value. This required between 0.5 and 1.5 ps: Longer trajectories were needed to achieve convergence of the constraint force close to the transition state (TS). In this way, the reaction coordinate was gradually decreased from 1.86 Å (M2 state) to 0.987 Å (D2 or D3 states), i.e., the system was smoothly driven from the reactant to product.

Within this approach, the free energy difference between states q_a and q_b is obtained by integrating the mean constraint force along q:[33]

$$\Delta G = -\int_{q_a}^{q_b} dq' \langle f \rangle_{q'} . \tag{1}$$

This method, in conjunction with CP molecular dynamics, has been successfully applied to study many reactive processes in complex systems.[22,23,34–39] It is generally more efficient than performing a constrained (0 K) structure optimization at each point along the reaction path, because the convergence of the mean force is usually fast, i.e., relatively short trajectories are required. Moreover, the finite temperature allows to include entropic and anharmonic effects explicitly, and a reliable estimate of the free energy is obtained, provided a meaningful reaction coordinate is selected.[22]

The mean constraint force and its integral are shown in Fig. 4. The q value corresponding to the TS can be located as the point in which the mean constraint force changes sign.[35] Looking at Fig. 4 this occurs at $q_{TS} \sim 1.25$ Å. We checked that this is a reliable TS by starting two unconstrained MD trajectories from the q points closest to it, on the reactant and product sides. In both cases the free dynamics led to the corresponding molecular or dissociated species in a very short time. The activation free energy for the dissociation ($\Delta G^{\ddagger}$) is 0.1 eV. As a further consistency check, a constrained geometry optimization with $q = q_{TS}$ was carried out. The adsorption energy of the resulting structure (labeled TS in Fig. 6) is 1.35 eV, corresponding to a potential energy barrier of 0.12 eV, close to the free energy barrier. Besides confirming the accuracy of the free energy calculations, this allow estimating a low entropy difference: $\Delta S^{\ddagger} \sim 6.7 \times 10^{-5}$ eV/K.

For $q < q_{TS}$, the mean force is large and negative, indicating that the proton is strongly attracted by the surface oxygen.[36] When $q = 1.03$ Å, the mean force is still large due to the O_{2c}–H bond being constrained to a value larger to the equilibrium bond distance. In the last constrained trajectory, q has been chosen equal to the O_{2c}–H bond distance in the D3 structure (0.987 Å). The mean force decays to zero, showing that an equilibrium configuration was reached. In this last run, the expected migration of O_tH to the vacancy was completed in 1.4 ps.

The dissociation free energy (ΔG_{diss}) that we obtain from this calculation (−0.107 eV) is smaller, in absolute value, than the potential energy difference between the molecular M2 and the dissociated D3 state. In fact, during the constrained dynamics towards the products, before reaching the final equilibrium state, the system probes many configurations corresponding to the metastable dissociated D2 state, whose potential energy is very close to the one of the molecular state M2. As the free energy basin of the products includes configurations close to either D2 and D3 minima, it will receive a (potential energy) contribution from both. Indeed the chosen reaction coordinate, while suitable to follow the proton transfer up to the TS, cannot discern between D2 and D3 states. A different reaction coordinate, like the distance between the water oxygen and O_{2c}, would be more suitable in this context, but presumably not so effective in describing the proton transfer. The point is that a single constraint is in some cases not enough to control the full reaction path from reactants to products.[35,36,40] The reaction coordinate that we choose is most effective for evaluating the free energy barrier, which is our main interest in this work. We also note that some positive entropic contribution to ΔG_{diss} cannot be ruled out, but it is unlikely that they are the sole responsible of the observed difference between free and potential energy of dissociation.

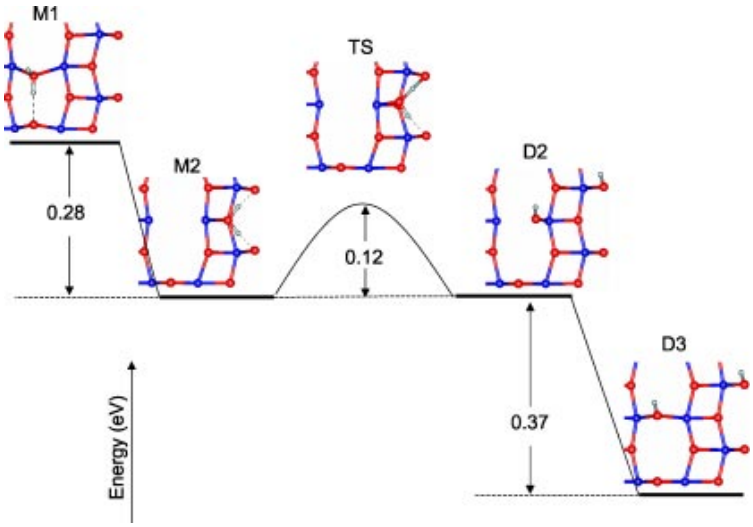

FIG. 6. Potential energy diagram for the proposed water dissociation path. Labels as in Figs. 2 and 3.

IV. DISCUSSION AND CONCLUSIONS

The kinetic rate constant can be estimated by the transition-state theory (TST) expression:

$$k = \frac{k_B T}{h} e^{-\Delta G^{\ddagger}/k_B T}, \tag{2}$$

where k_B and h are Boltzmann's and Planck's constants, respectively. Equation (2) yields $k = 0.11\ \mathrm{ps}^{-1}$ at 300 K. Thus, it is *a posteriori* not surprising that no dissociation of the molecular M2 configuration was observed in the above-mentioned 6 ps unconstrained trajectory at 300 K. As a consistency check, we performed a further MD simulation in which, after raising the temperature to ~700 K, we let the system evolve without constraints. We found that after only 0.2 ps a water proton moved to an O_{2c} (Fig. 5); the transfer was followed by two quick recombinations, with the proton moving between the two oxygens, before ending in the dissociated state. Then the migration of the terminal hydroxyl to the vacancy takes place, as shown by the increase of the O_w–H distance in Fig. 5.

A possible mechanism for the dissociation of water adsorbed at low coverage on defective anatase (101) can be sketched on the basis of these findings (see Fig. 6). Molecular adsorption on Ti_{4c} is favored initially. It can in principle occur in two different modes: With the water oxygen roughly replacing the missing bridging oxygen (M1) or in the more stable mode M2. A direct dissociation of the molecule inside the vacancy[21] is unlikely: Molecular migration from M1 to the other stable site is observed instead. Dissociation of water in this site, leading to a terminal and a bridging hydroxyl, is practically thermoneutral. The driving force of the dissociative process is the subsequent migration of the OH_t to the vacancy site, leading to a more stable dissociated state with two bridging hydroxyls (D3). While the last diffusive process is spontaneous at $T = 300$ K, the initial proton transfer to a surface O_{2c} requires the crossing of a somewhat larger barrier. Whereas this barrier is high enough to hinder the dissociation on the time scales available by *ab initio* molecular dynamics, on macroscopic time scales it is likely that all water molecules near vacancy sites are dissociated at low coverage.

In conclusion, our first principles molecular-dynamics simulations have elucidated the dissociation pathway of a water molecule adsorbed close to a low-coordinated defect site on the TiO_2 anatase (101) surface. We have found that the dissociation does not follow a direct pathway. Even though the overall barrier is small, the process is complex, involving a few different intermediate states.

ACKNOWLEDGMENTS

The calculations of this work have been performed on the Lemieux Terascale Computing System at the Pittsburgh Supercomputer Center and on the IBM-SP3 computer at the Keck Computational Materials Science Laboratory in Princeton. We acknowledge support by the National Science Foundation under Grant No. CHE-0121432.

[1] A. L. Linsebigler, G. Lu, and J. T. Yates, Chem. Rev. **95**, 735 (1995).
[2] M. R. Hoffmann, S. T. Martin, W. Choi, and D. W. Bahnemann, Chem. Rev. **95**, 69 (1995).
[3] G. E. Brown, Jr., V. E. Henrich, W. H. Casey *et al.*, Chem. Rev. **99**, 77 (1999).
[4] M. A. Henderson, Surf. Sci. Rep. **46**, 1 (2002).
[5] M. A. Henderson, W. S. Epling, C. H. F. Peden, and C. L. Perkins, J. Phys. Chem. B **107**, 534 (2003).
[6] M. B. Hugenschmidt, L. Gamble, and C. T. Campbell, Surf. Sci. **302**, 329 (1994).
[7] M. A. Henderson, Surf. Sci. **355**, 151 (1996).
[8] S. P. Bates, G. Kresse, and M. J. Gillan, Surf. Sci. **409**, 336 (1998).
[9] P. J. D. Lindan, N. M. Harrison, J. M. Holender, and M. J. Gillan, Chem. Phys. Lett. **261**, 246 (1996).
[10] P. J. D. Lindan, N. M. Harrison, and M. J. Gillan, Phys. Rev. Lett. **80**, 762 (1998).
[11] E. V. Stefanovich and T. N. Truong, Chem. Phys. Lett. **299**, 623 (1999).
[12] I. M. Brookes, C. A. Muryn, and G. Thornton, Phys. Rev. Lett. **87**, 266103 (2001).
[13] R. Schaub, P. Thorstrup, E. Laegsgaard, I. Steensgaard, J. K. Nørskov, and F. Besenbacher, Phys. Rev. Lett. **87**, 266104 (2001).
[14] L. Kavan, M. Grätzel, S. E. Gilbert, C. Klemenz, and H. J. Scheel, J. Am. Chem. Soc. **118**, 6716 (1996).

[15] M. Lazzeri, A. Vittadini, and A. Selloni, Phys. Rev. B **63**, 155409 (2001).
[16] A. Vittadini, A. Selloni, F. P. Rotzinger, and M. Grätzel, Phys. Rev. Lett. **81**, 2954 (1998).
[17] G. S. Herman, Z. Dohnálek, N. Ruzycki, and U. Diebold, J. Phys. Chem. B **107**, 2788 (2003).
[18] W. Hebenstreit, N. Ruzycki, G. S. Herman, Y. Gao, and U. Diebold, Phys. Rev. B **62**, R16334 (2000).
[19] R. Car and M. Parrinello, Phys. Rev. Lett. **55**, 2471 (1985).
[20] W. Langel and M. Parrinello, J. Chem. Phys. **103**, 3240 (1995).
[21] W. Langel, Surf. Sci. **496**, 141 (2002).
[22] K. C. Haas, W. F. Schneider, A. Curioni, and W. Andreoni, Science **282**, 265 (1998).
[23] K. C. Haas, W. F. Schneider, A. Curioni, and W. Andreoni, J. Phys. Chem. B **104**, 5527 (2000).
[24] M. Odelius, Phys. Rev. Lett. **82**, 3919 (1999).
[25] J. P. Perdew, K. Burke, and M. Ernzerhof, Phys. Rev. Lett. **77**, 3865 (1996).
[26] D. Vanderbilt, Phys. Rev. B **63**, 155409 (1990).
[27] A. Vittadini, A. Selloni, F. P. Rotzinger, and M. Grätzel, J. Phys. Chem. B **104**, 1300 (2000).
[28] A. Vittadini and A. Selloni, J. Chem. Phys. **117**, 353 (2002).
[29] M. Ramamoorthy, R. D. King-Smith, and D. Vanderbilt, Phys. Rev. B **49**, 7709 (1994).
[30] P. J. D. Lindan, N. M. Harrison, M. J. Gillan, and J. A. White, Phys. Rev. B **55**, 15919 (1997).
[31] M. A. Henderson, W. S. Epling, C. L. Perkins, C. H. F. Peden, and U. Diebold, J. Phys. Chem. B **103**, 5328 (1999).
[32] E. A. Carter, G. Ciccotti, J. T. Hynes, and R. Kapral, Chem. Phys. Lett. **156**, 472 (1989).
[33] M. Sprik and G. Ciccotti, J. Chem. Phys. **109**, 7737 (1998).
[34] A. Curioni, M. Sprik, W. Andreoni, H. Schiffer, J. Hütter, and M. Parrinello, J. Am. Chem. Soc. **119**, 7218 (1997).
[35] E. J. Meijer and M. Sprik, J. Am. Chem. Soc. **120**, 6345 (1998).
[36] S. Raugei and M. Klein, J. Phys. Chem. B **106**, 11596 (2002).
[37] C. Mundy, J. Hutter, and M. Parrinello, J. Am. Chem. Soc. **122**, 4837 (2000).
[38] B. L. Trout and M. Parrinello, J. Phys. Chem. B **103**, 7340 (1999).
[39] A. Tilocca, M. A. Vanoni, A. Gamba, and E. Fois, Biochemistry **41**, 14111 (2002).
[40] M. Mugnai, G. Cardini, and V. Schettino, J. Phys. Chem. A **107**, 2540 (2003).